Royal Norwegian Council
for Scientific and Industrial Research
(NTNF)

NORSAR

NORSAR Scientific Report No. 1-91/92

Semiannual Technical Summary

1 April — 30 September 1991

Kjeller, November 1991

7.5 Initial testing of mixed event separation using a statistically optimal adaptive algorithm.

Introduction

The network of the three Fennoscandian regional arrays, ARCESS, FINESA and NORESS, has shown an excellent capability to monitor the seismic activity at the Soviet test site at Novaya Zemlya. In a previous report (Kværna and Ringdal, 1990), we demonstrated the application of the threshold monitoring (TM) technique to obtain continuous estimates of the largest size of events that might go undetected by the monitoring network. This study showed that during normal noise conditions, it was possible to monitor the Novaya Zemlya test site in this way down to m_b 2.5 more than 99% of the time.

However, during intervals of increased seismic amplitude levels at the arrays, e.g., caused by the arrivals of signals from strong earthquakes, the monitoring capability may deteriorate significantly, as shown in Fig. 7.5.1. For the day analyzed in Fig. 7.5.1, a maximum network threshold of 3.8 occurred because of arrivals from a strong earthquake at Hindu Kush (m_b = 6.0). This implies that an event of magnitude 3.8 in theory could have occurred at Novaya Zemlya at that time without exceeding the network threshold.

To improve the monitoring capability during such intervals of increased magnitude thresholds, we have started to evaluate the potential of a statistically optimal processing scheme (Kushnir and Lapshin, 1984) for suppressing the effect of interfering coherent arrivals. The method, denoted adaptive optimal group filtering (AOGF), has earlier been applied for extraction of signals from background noise (Kushnir et al., 1990). Compared to conventional beamforming at NORESS and ARCESS, AOGF has demonstrated a capability to provide significant SNR gains over a wide frequency band (0.2-5.0 Hz). The largest gain (12-18 dB more than conventional beamforming) is obtained at low frequencies where the method utilizes the very coherent nature of the noise. But even for the frequency band from 2 to 4 Hz, AOGF provides a typical SNR gain of the order of 6 to 8 dB compared to the conventional beam.

Theoretical background for adaptation to interfering events

In the study of Kushnir et al. (1990), a pure noise interval preceding the signal was selected for adaptation. Exploiting the stationarity of the background noise field, the interval containing the signal was subsequently processed by the AOGF method using the parameters obtained during the adaptation.

This procedure is, however, *not* relevant when we want to extract a hypothetical signal hidden somewhere in the coda of another signal. In this case, we do *not* know *if* or *when* the hypothetical event occurred, and do only have information on the slowness and azimuth of the hypothetical signal. For AOGF to be applicable to our new purpose, the adaptation needs to be successful even if the adaptation interval contains the wave we want to extract.

We will in the following show theoretically that the AOGF method has the desired property:

The AOGF method is based on an optimal Wiener group filter (OGF) with frequency response:

$$\vec{g}(f) = (g_1(f), \ldots, g_m(f)) \tag{1}$$

where m is the number of array sensors.

The OGF has the characteristics of effectively suppressing the coherent part of the noise field while keeping the signature of the wanted plane wave undistorted. The filter $\vec{g}(f)$ transforms the input array data $\vec{x}_t = (x_{1t}, \ldots, x_{mt})^T$ (where T denotes the transpose) into a scalar trace y_t. $y_t = \vec{g}_t * \vec{x}_t$ where * denotes convolution, and $y(f) = \vec{g}(f) \cdot \vec{x}(f)$, where $y(f)$, $\vec{g}(f)$ and $\vec{x}(f)$ are the Fourier transforms of y_t, $\vec{g}_t$ and $\vec{x}_t$.

It is well known that $\vec{g}(f)$ has the form:

$$\vec{g}(f) = \frac{\vec{h}^{\dagger}(f) \cdot F_n^{-1}(f)}{\vec{h}^{\dagger}(f) \cdot F_n^{-1}(f) \cdot \vec{h}(f)} \tag{2}$$

where $F_n(f)$ is the power spectral density matrix of the noise $\vec{n}_t = (n_{1t}, \ldots, n_{mt})^T$. $\vec{h}(f) = (h_1(f), \ldots, h_m(f))^T$, where $h_k(f) = e^{-2\pi f T_k}$ and T_k is the time delay at the k^{th} sensor for the plane wave to be extracted from the background noise field. $\dagger$ denotes the Hermitian conjugate.

If we are adapting to a pure noise interval, the matrix $F_n^{-1}(f)$ is estimated by a special procedure. From a computational and statistical point of view,a good way to estimate the large size matrix $F_n^{-1}(f)$ is to use autoregressive modelling of the noise field $\vec{n}_t$. The new filter

$$\vec{g}(f) = \frac{\vec{h}^{\dagger}(f) \cdot \hat{F}_n^{-1}(f)}{\vec{h}^{\dagger}(f) \cdot \hat{F}_n^{-1}(f) \cdot \vec{h}(f)} \tag{3}$$

is referred to as the adaptive optimal group filter (AOGF) where $\hat{F}_n^{-1}(f)$ is the autoregressive estimate of $F_n^{-1}(f)$.

If the adaptation interval contains a mixture of the signal and pure noise, i.e., $\vec{x}_t = \vec{s}_t + \vec{n}_t$, we cannot estimate $F_n^{-1}(f)$ but only the spectral density matrix $F_x^{-1}(f)$ of the mixture. Let us consider the group filter

$$\vec{d}(f) = \frac{\vec{h}^{\dagger}(f) \cdot F_x^{-1}(f)}{\vec{h}^{\dagger}(f) \cdot F_x^{-1}(f) \cdot \vec{h}(f)} \tag{4}$$

where

$$F_x(f) = E\{[\vec{n}(f) + \vec{h}(f) z(f) e^{-2\pi i f T_0}] [\vec{n}(f) + \vec{h}(f) z(f) e^{-2\pi i f T_0}]^{\dagger}\}$$

$$= F_n(f) + \vec{h}(f) \vec{h}^{\dagger}(f) \cdot p(f)$$

and $z(f)$ is the Fourier transform of the signal waveform, T_0 is the travel-time to the reference sensor of the array, $p(f)$ is the power spectral density of the signal waveform and E denotes statistical expectation.

Using a formula of Bartlett (1951) for matrix inversion, we can write:

$$F_x^{-1}(f) = F_n^{-1}(f) - F_n^{-1}(f) \vec{h}(f) \vec{h}^{\dagger}(f) F_x^{-1}(f) p(f) \left[1 + \vec{h}^{\dagger}(f) F_x^{-1}(f) \vec{h}(f)\right]^{-1} \tag{5}$$

Substituting (5) into (4) yields:

$$\vec{d}(f) = \frac{\vec{h}^{\dagger}(f) \cdot F_n^{-1}(f)}{\vec{h}^{\dagger}(f) \cdot F_n^{-1}(f) \cdot \vec{h}(f)} \cdot \frac{I\left[1 - \vec{h}^{\dagger}(f) F_n^{-1}(f) \vec{h}(f) \cdot C\right]}{\left[1 - \vec{h}^{\dagger}(f) F_n^{-1}(f) \vec{h}(f) \cdot C\right]} = \vec{g}(f) \tag{6}$$

where I is the identity matrix and $C = p(f) \cdot \left[1 + \vec{h}^{\dagger}(f) F_n^{-1}(f) \vec{h}(f)\right]^{-1}$.

Equation (6) shows that in theory, AOGF will work even if the adaptation interval contains the plane wave we want to extract.

Processing of synthetic mixtures

The main problem arising when attempting to utilize the derived theoretical property of AOGF in data processing practice, is to estimate $F_x^{-1}(f)$ with sufficient accuracy using a mixture of signal and noise records. Autoregressive modelling in principle gives us such an opportunity. This will be shown in some experiments with simulated array data.

Using the geometry of the NORESS array, we have synthesized a mixture of a transient plane wave and a stationary coherent noise field with some added white noise. The slowness vector of the modelled transient is identical to that of a P-wave originating at the Novaya Zemlya test site. With relevance to the problem case outlined in the introduction, the slowness vector of the stationary coherent noise field corresponds to that of a P-wave from an event in the Hindu Kush region. Using the current implementation of the AOGF method, a successful signal extraction is shown in Fig. 7.5. 2. The conventional beam shown on the top trace did not reveal the signal, whereas the signal clearly stands out on the AOGF filtered trace shown in the middle. For comparison, a single array sensor is shown at the bottom. This experiment shows that the current AOGF implementation is

capable of extracting a simple signal from a simple noise field, even if adaptation is made to the data containing the signal we want to extract.

Experiments with NORESS data with a real Novaya Zemlya signal superimposed in the coda of a real Hindu Kush event did not give the desirable result with the current implementation of the AOGF method. This can be explained by the specific features of the software, which has been designed for on-line implementation, as shown by Kushnir et al. (1990). In this program, adaptation is made after steering the array to the chosen direction, resulting in synchronized signal waveforms when data contain the signal we want to extract. Our working hypothesis is that this creates a problem for the multichannel autoregressive estimation procedure, in particular if the background noise has rather complex spatial features like an earthquake coda.

An additional experiment indicates that if we introduce the appropriate changes to the AOGF implementation (by doing all computations in the frequency domain without steering of the array sensors), a successful signal extraction can be achieved, even in the case when the adaptation interval contains a real seismic signal superimposed in the coda of another seismic event.

The experiment, simulating the frequency domain version of AOGF by use of the current AOGF software, consisted of the following steps:

1. A synthetic mixture was created by superimposing down-scaled records of the Novaya Zemlya explosion of 24 October 1990 in the coda of a real Hindu Kush event (event 1 of Table 7.5.1). The SNR between the Novaya Zemlya and the Hindu Kush signals was approximately 1.
2. Adaptation to this data was made without introducing time delays (steering with infinite apparent velocity), thus avoiding synchronized waveforms.
3. A new synthetic mixture was created by superimposing a transient plane wave with infinite apparent velocity and the waveform of the Novaya Zemlya explosion in the coda of the Hindu Kush event. In this case the SNR was only 0.25.
4. This data was then AOGF filtered with the parameters obtained during the previous adaptation.

The result is given in Fig. 7.5.3, indicating the successful extraction of the signal.

This procedure is similar to what will be done by the new frequency-domain implementation of AOGF, thus indicating that the theoretical property outlined in the preceding section, may also be valid in practice.

Adaptation to a neighboring event

We have also investigated the possibility of using two neighboring events in the AOGF processing, using one event for adaptation, and subsequently AOGF filtering the other event (which may contain another signal) with the parameters obtained during the adaptation to the first event.

Two strong Hindu Hush earthquakes with an epicentral difference of approximately 100 km were chosen for this experiment (see Table 7.5.1). The first 20 seconds of the two P-wavetrains recorded at NORESS are shown in Fig. 7.5.4, and the spectra of the first 10 seconds are given in Fig. 7.5.5. Note that the spectra show very similar characteristics.

The results of this test are summarized in the spectra of Fig. 7.5.6. The upper curve shows the spectrum of a conventional beam steered with a slowness vector corresponding to a P-wave from the Novaya Zemlya test site, using NORESS data for Hindu Kush event no. 1 (see Table 7.5.1). The spectrum shown by the solid line below, corresponds to the AOGF beam steered to Novaya Zemlya of Hindu Kush event no. 1, using Hindu Kush event no. 2 for adaptation; and the spectrum shown by the dashed line, corresponds to the AOGF beam steered to Novaya Zemlya of Hindu Kush event no. 1, using the same event (no. 1) for adaptation.

Comparing the spectra suggests that for frequencies below 1 Hz, the AOGF method can suppress the effect of interfering events much better than conventional beamforming, when a neighboring event has been used for adaptation. For higher frequencies, the improvement is also significant. The spectrum shown by the dashed line, indicate that more improvement can be obtained if the same event is used for adaptation.

To visualize the effect of using a neighboring event for adaptation, we superimposed records of the down-scaled Novaya Zemlya explosion in the coda of Hindu Kush event no. 1. As in Fig. 7.5.3, the SNR was 0.25. The results from AOGF filtering this mixture signal with the adaptation parameters retrieved from Hindu Kush event no. 2., are shown in the middle trace of Fig. 7.5.7. As expected, due to signal loss during the plane-wave beam-forming, the amplitude of the Novaya Zemlya signal is reduced with comparison to the amplitude of Fig. 7.5.3. Also indicated by the spectra of Fig. 7.5.6, the amplitude of the Hindu Kush event is not as effectively suppressed as in the case of Fig. 7.5.3, but we are still able to identify the Novaya Zemlya arrival on the AOGF beam.

To further compare the relative performance between the conventional and the AOGF beams, we bandpass filtered the traces of Fig. 7.5.7 in the frequency band providing the largest SNR (i.e., 1.5-3.5 Hz). The results are shown in Fig. 7.5.8. The only difference from Fig. 7.5.7, is that instead of using all sensors of the NORESS array when forming the conventional beam, we used a sub-geometry consisting of A0Z, the C-ring and the D-ring (17 sensors). In the frequency band 1.5-3.5 Hz, this sub-geometry will provide the best SNR improvement, at least when comparing to background noise conditions (Kværna, 1989). The result shows that when using a neighboring event for adaptation, the AOGF beam provides better SNR than the optimum conventional beam (optimum = best sub-geometry and best filter band).

Discussion

The results presented above suggest that application of the AOGF method has a potential for significantly improving the signal-to-noise ratios of seismic events occurring in the coda of large earthquakes. This is important, e.g., for improving the threshold monitoring capability during periods of increased magnitude thresholds. The experiments with the

Hindu Kush events recorded at NORESS indicate that with the appropriate changes to the AOGF software (by implementing the frequency domain version), a significant threshold magnitude reduction may be achieved for each phase considered.

Applying the software currently available, using adaptation to a neighboring event, we have the capability of some reduction of the magnitude thresholds.

The continuation of this research will consist of carefully testing the frequency-domain version of AOGF, and special emphasis will be devoted to ensuring the undistorting feature of AOGF on the signal we want to extract from the background coda. In addition, practical problems related to the use of AOGF in the threshold monitoring algorithm will be investigated.

Tormod Kværna
Alex Kushnir, MITPAN Institute, Moscow, USSR

References

Bartlett, M.S. (1951): In inverse matrix adjustment, arising in discriminant analysis, *Ann. Math. Stat.*, Vol. 2, No. 1

Kushnir, A.F., J. Fyen and T. Kværna (1990): Multichannel statistical data processing algorithms in the framework of the NORSAR event processing program package, *Semiannual Tech. Summary, 1 Oct 1990 - 31 Mar 1991*, NORSAR Sci. Rep. 2-90/91, NORSAR, Kjeller, Norway.

Kushnir, A. F. and V. M. Lapshin (1984): Optimal processing of the signals received by a group of spatially distributed sensors, in *Computational Seismology*, Allerton Press, Inc., Vol 17, 163-174.

Kværna, T (1989): On exploitation of small-aperture NORESS type arrays for enhanced P-wave detectability, *Bull. Seism. Soc. Am.* 79, 888-900.

Kværna, T. and F. Ringdal (1990): Continuous threshold monitoring of the Novaya Zemlya test site, *Semiannual Tech. Summary, 1 Apr - 30 Sep 1990*, NORSAR Sci. Rep. 1-90/91, NORSAR, Kjeller, Norway.

Event no.	Year	Day	Mon	Or.time	Lat	Lon	Depth	m_b
1	1990	25	Oct	04.53.59.9	35.121N	70.486E	114	6.0
2	1990	15	May	14.25.20.6	36.043N	70.428E	113	5.9

Table 7.5.1. PDE locations of the Hindu Kush events.

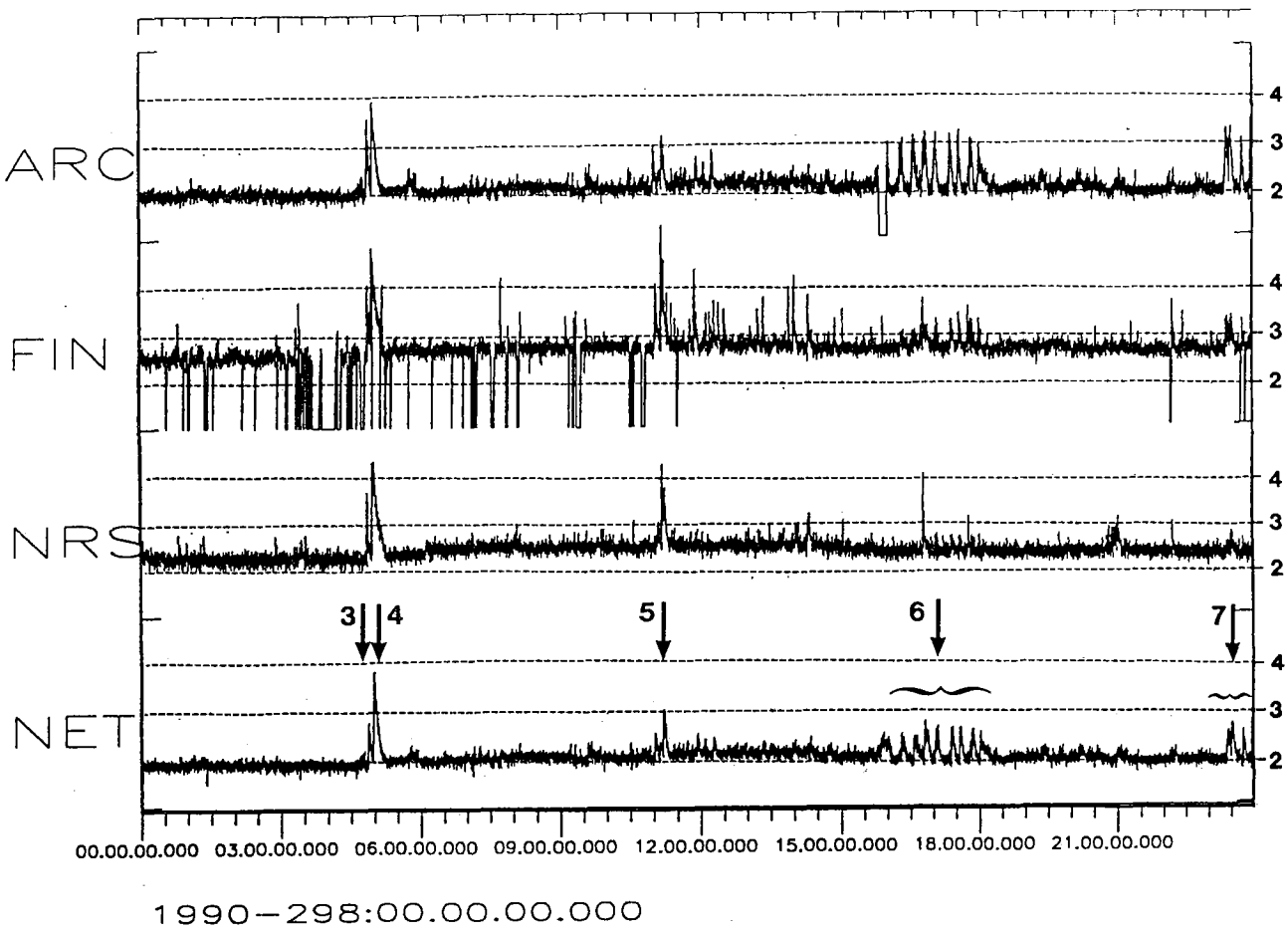

Fig. 7.5.1. Threshold monitoring of the Novaya Zemlya test site for day 298(25 October 1990). The top three traces represent thresholds (upper 90 per cent magnitude limits) obtained from each of the three arrays (ARCESS, FINESA, NORESS), whereas the bottom trace shows the combined network thresholds. The FINESA array had several short outages this day, but this caused no particular problems in terms of network threshold capacity.

Notes:

3. An earthquake (m_b = 4.5) near Jan Mayen. The corresponding network threshold peak for Novaya Zemlya is m_b = 2.8.
4. A teleseismic earthquake (m_b = 6.0) at Hindu Kush. The relatively strong P-wave train caused a peak threshold of m_b = 3.8 for monitoring Novaya Zemlya.
5. A teleseismic earthquake (m_b = 5.9) at Mindanao, Philippine Islands. Corresponding threshold is m_b = 3.0.

6.-7. A sequence of seismic events (presumably underwater explosions) near Murmansk, Kola Peninsula. The network threshold for monitoring Novaya Zemlya is about m_b = 2.5 to 2.8 at the times of these events.

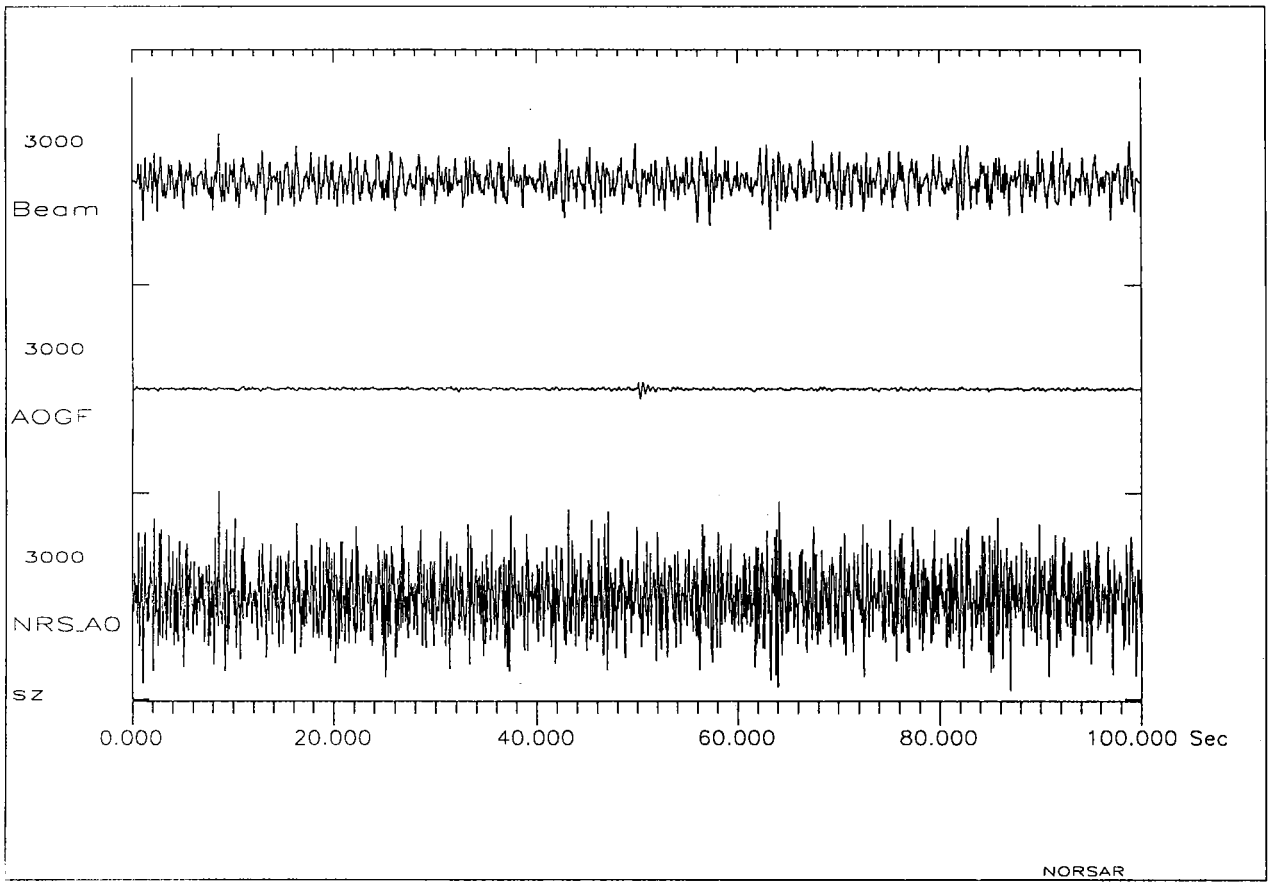

Fig. 7.5.2. Synthetic processing example.
A synthetic signal has been created by adding three components as follows:

1) A stationary, coherent noise field (Hindu Kush direction, P velocity).
2) A stationary, incoherent "white noise" field.
3) A transient, coherent signal (Novaya Zemlya direction, P velocity).

The top trace shows the conventional beam steered to Novaya Zemlya.
The middle trace shows the AOGF beam steered to Novaya Zemlya.
The bottom trace shows the single sensor A0Z.

Note that the signal is clearly visible on the AOGF trace, but not on the other two.

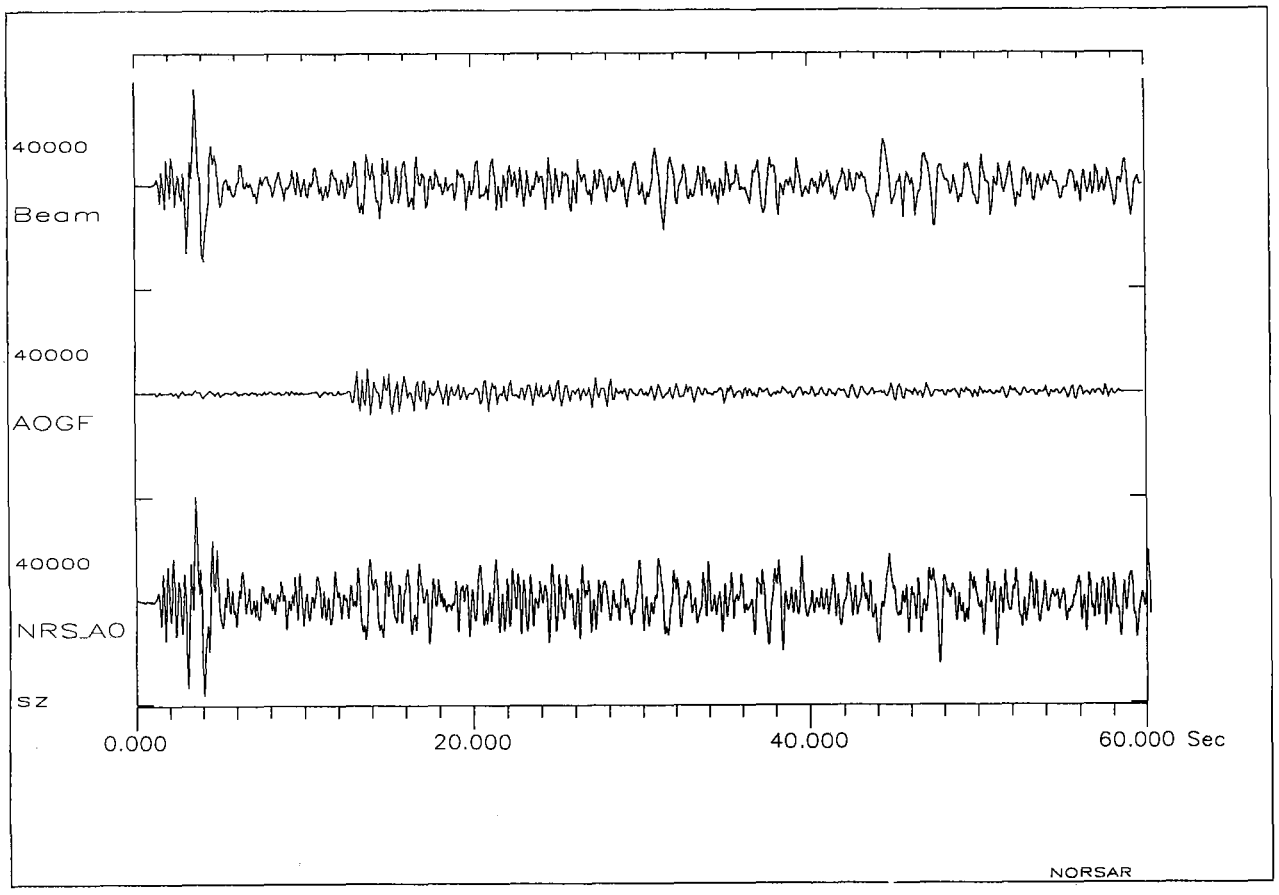

Fig. 7.5.3. Synthetic processing example, illustrating that with the appropriate changes to the AOGF program, we may have the possibility of extracting a real seismic signal from an earthquake coda, even if the adaptation interval containing the signal we want to extract.

The experiment, simulating the frequency domain implementation of AOGF, consisted of the following steps:

1) A synthetic mixture was created by superimposing down-scaled records of the Novaya Zemlya explosion of 24 October 1990 in the coda of a real Hindu Kush event (event 1 of Table 7.5.1). The SNR between the Novaya Zemlya and the Hindu Kush signals was approximately 1.

2) Adaptation to this data was made without introducing time delays (steering with infinite apparent velocity), thus avoiding synchronized waveforms.

3) A new synthetic mixture was created by superimposing a transient plane wave with infinite apparent velocity and the waveform of the Novaya Zemlya explosion in the coda of the Hindu Kush event. In this case the SNR was only 0.25.

4) This data was then AOGF filtered with the parameters obtained during the previous adaptation.

The top trace shows the conventional beam steered with infinite apparent velocity.
The middle trace shows the AOGF beam steered with infinite apparent velocity.
The bottom trace shows the single sensor A0Z.

Note that the signal is clearly visible on the AOGF trace, but not on the other two.

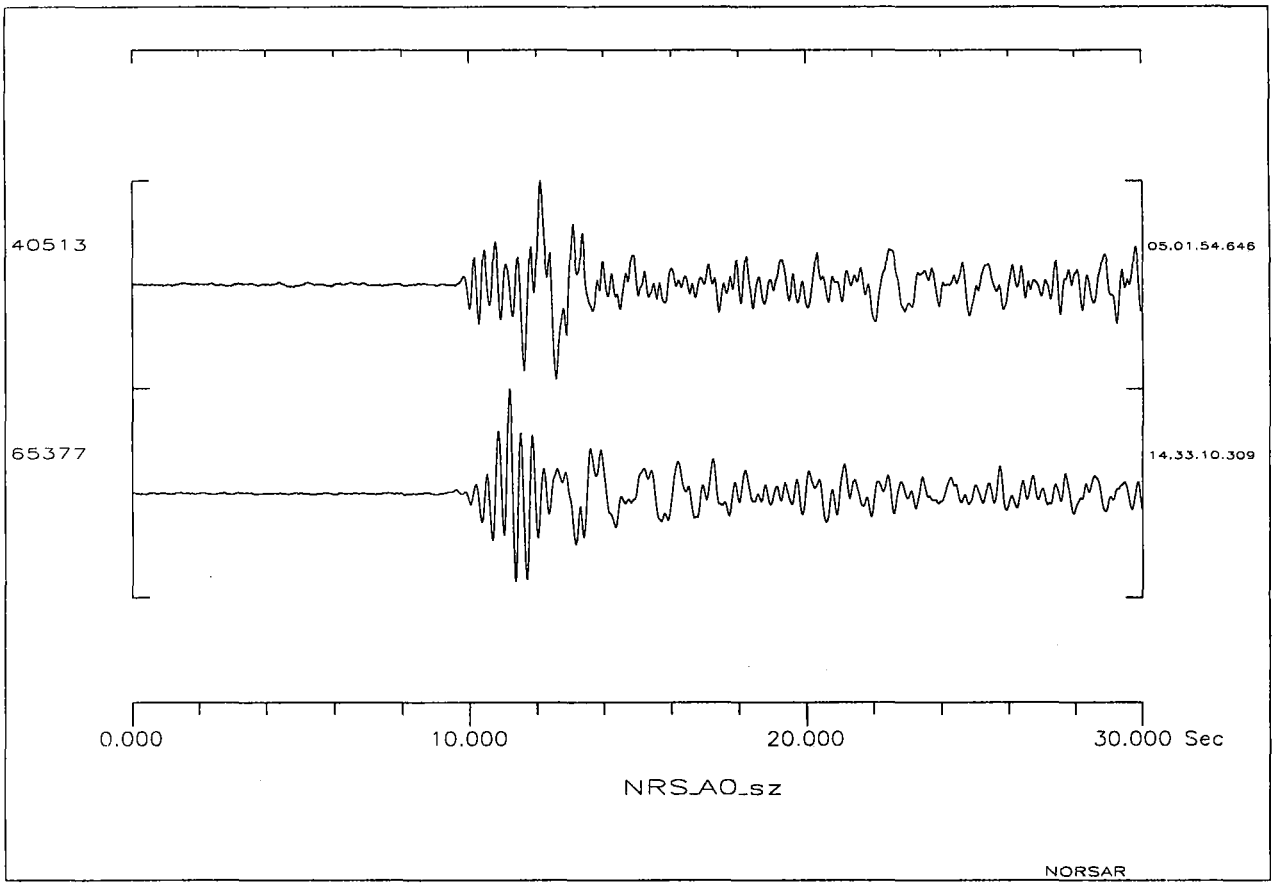

Fig. 7.5.4. NORESS recordings (instrument A0Z) of the two Hindu Kush events described in Table 7.5.1. Event no. 1 is shown in the upper trace, and event no. 2 in the lower.

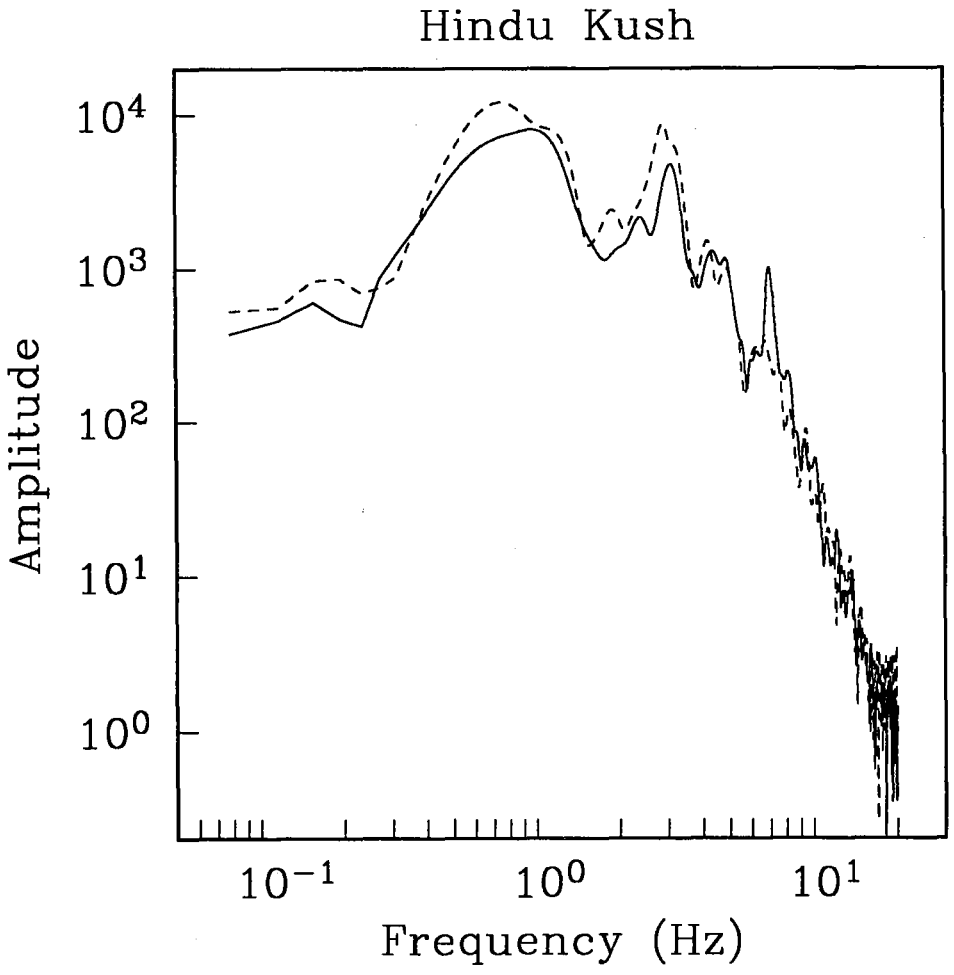

Fig. 7.5.5. P-wave spectra of NORESS recordings of the two Hindu Kush events described in Table 7.5.1. Solid line: Event no. 1. Dashed line: Event no. 2. Both spectra were estimated using 10 seconds of data.

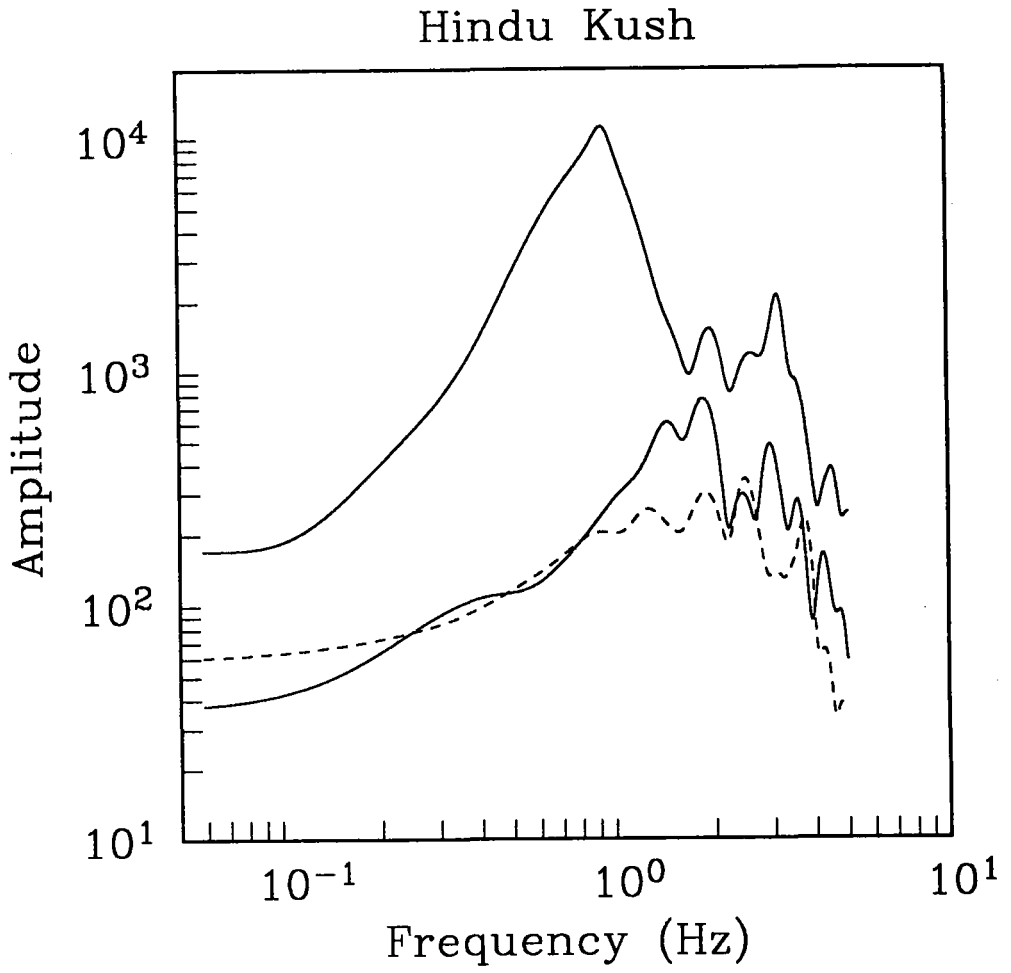

Fig. 7.5.6. After processing Hindu Kush event no. 1 with different techniques, we computed P-wave amplitude spectra of the first 10 seconds of the signal. The upper spectrum results from conventional beamforming using the Novaya Zemlya P-wave steering delays. The lower solid line spectrum results from AOGF filtering with Novaya Zemlya P-wave steering delays using Hindu Kush event no. 2 for adaptation. The dashed line spectrum results from AOGF filtering with Novaya Zemlya P-wave steering delays using the same event (no. 1) for adaptation.

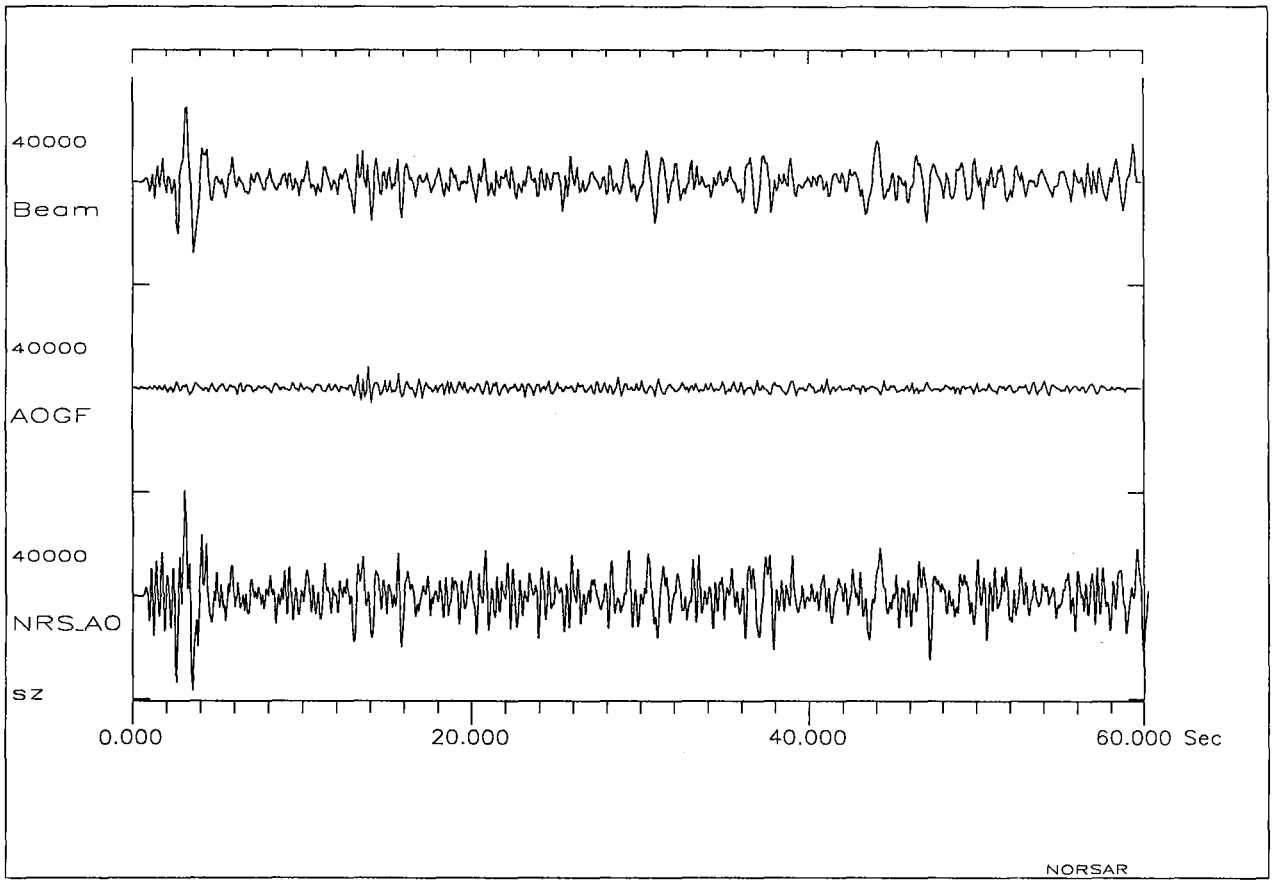

Fig. 7.5.7. Results after processing the mixture of Hindu Kush event no. 1 and the down-scaled Novaya Zemlya signal. Single channel SNR ~ 0.25. The lower trace shows a single NORESS sensor, the top trace is a conventional beam steered to Novaya Zemlya, whereas the middle trace is the AOGF output using Hindu Kush event no. 2 for adaptation.

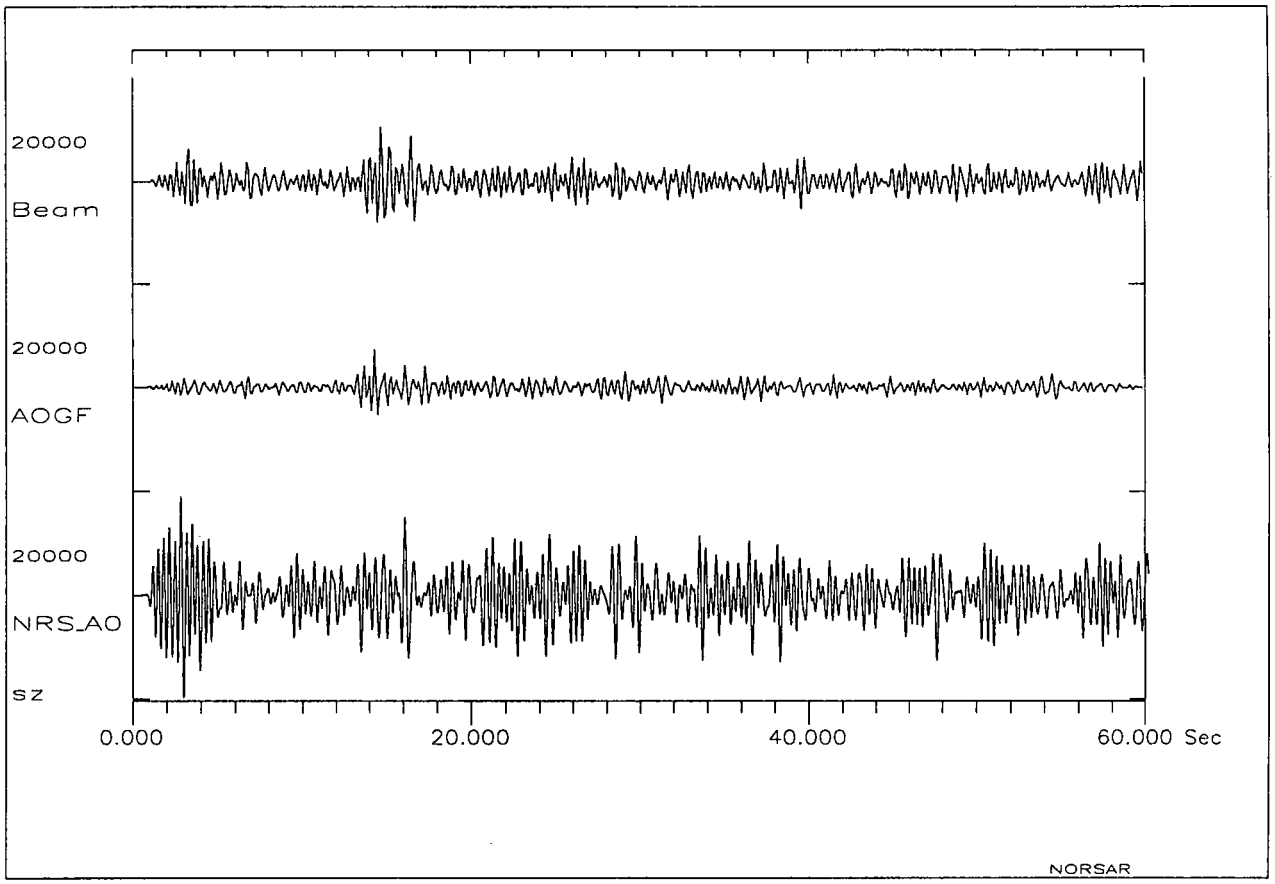

Fig. 7.5.8. Results from bandpass filtering the data of Fig. 7.5.7 in the passband 1.5-3.5 Hz. The only difference from Fig. 7.5.7, is that instead of using all sensors of the NORESS array when forming the conventional beam, we used a sub-geometry consisting of A0Z, the C-ring and the D-ring (17 sensors). Note that even under these optimum conditions for conventional beamforming, the AOGF beam provide the best SNR.